Estimation of Bloch Model MT Spin System Parameters from Z-Spectral Data

R. W. Holt, J. L. Duerk, J. Hua, G. C. Hurst

Previous studies have described magnetization transfer (MT) Z-spectra in terms of a two-pool Bloch model, with six spin-system parameters K_A, F, T_{1A}, T_{1B}, T_{2A}, and T_{2B}. By simulation, we show that a process including nonlinear constrained optimization can be used to accurately and uniquely estimate spin-system parameters from MT Z-spectra prepared by continuous wave (CW) RF irradiation. Experiments producing Z-spectra by pulsed RF irradiation give substantially different magnetization values, relative to MT acquisitions obtained by CW RF irradiation, at small offset frequencies, with a consequence that only T_{2B} can be uniquely determined. However, several equalities and bounds involving four of the other parameters (K_A, F, T_{1A}, and T_{1B}) are derived, which are applicable to pulsed data. These relationships allow calculation of "free pool" magnetization corresponding to complete saturation of the restricted pool, without requiring that this complete saturation be experimentally achieved. MT experimental data from pulsed RF irradiation on boiled egg albumin, obtained using a clinical whole-body MRI system, are analyzed using an optimization algorithm and the derived expressions.

Key words: magnetization transfer; Bloch model; spin parameters; optimization.

INTRODUCTION

Previous reports have presented measurements of two-pool magnetization transfer (MT) spin-system parameters using expressions derived from the Bloch equations and data from "Z-Spectra" (1–3). Spin-system parameters are estimated in those studies by either iterative fitting to simultaneously determine all six parameters (2), or "direct" calculation of T_{2B} from the positive (1) or negative (3) of intercept data regression lines. This report describes: a) the sensitivity of nonlinear constrained optimization (NLCO) (4, 5) when used to estimate these parameters; b) a novel analytic, linear relationship for Z-spectral data in terms of MT spin-system parameters; c) a synopsis of a method to measure T_{2B} from the negative intercept of data regression lines of $\Delta\omega^2$ and ω_1^2 at different Z-values (3, 6); and d) algebraic relationships between T_{2B} and four of the five remaining independent parameters (K_A, F, T_{1A}, and T_{1B}) applicable to Z-spectral data from the offset frequency range of greatest likely practical interest (e.g., 2 to 10 KHz).

MRM 31:122–130 (1994)

From the Departments of Radiology (R.W.H., J.L.D. J.H., G.C.H.), Biomedical Engineering (R.W.H., J.L.D.), and Chemistry (J.H., G.C.H.), MetroHealth Medical Center, and Case Western Reserve University, Cleveland, Ohio.

Address correspondence to: Gregory C. Hurst, Ph.D., Department of Radiology, MetroHealth Medical Center, 2500 MetroHealth Drive, Cleveland, OH 44109–1998.

Received August 2, 1993; revised September 29, 1993; accepted October 4, 1993.

Accepted for presentation at the 1993 Poster Sessions at the SMRM Annual Meeting and presented at the Joint SMRM/SMRI Symposium on Magnetization Transfer Contrast in MRI.

0740-3194/94 $3.00

DERIVATIONS AND SIMULATIONS

Starting Expressions and Derivations

As a starting point for our analysis, we use Wu's analytic expression for the steady-state longitudinal magnetization for the observed ("free") spin pool A (7):

$$Z = \frac{1}{2}\left(1 - \frac{M_A^{z}}{M_A^{z0}}\right) = \frac{A\omega_1^4\, B\omega_1^2\Delta\omega^2 + C\omega_1^2}{2[A\omega_1^4 + D\omega_1^2\Delta\omega^2 + E\Delta\omega^4 + G\omega_1^2 + H\Delta\omega^2 + I]} \quad [1]$$

This description of the Z-spectrum lineshape is based on a Bloch-equation model of two spin pools A and B coupled by cross-relaxation, with lettered coefficients defined by physical constants of spin pools A and B:

$$\begin{aligned}
A &= R_{2A}FT_{1A}T_{1B}R_{2B} \\
B &= R_{2A}T_{1A}(F + K_AT_{1B}) + FK_AT_{1A}T_{1B}R_{2B} \\
C &= R_{2A}R_{2B}T_{1A}[R_{2A}FK_AT_{1B} + R_{2B}(F + K_AT_{1B})] \\
D &= R_{2A}T_{1A}(F + K_AT_{1B}) + FT_{1B}R_{2B}(K_AT_{1A} + 1) \\
E &= FK_AT_{1A} + F + K_AT_{1B} \\
G &= R_{2A}R_{2B}[(R_{2A}FT_{1B}(K_AT_{1A} + 1) + T_{1A}R_{2B}(F + K_AT_{1B})] \\
H &= (R_{2A}^2 + R_{2B}^2)(FK_AT_{1A} + F + K_AT_{1B}) \\
I &= R_{2A}^2R_{2B}^2(FK_AT_{1A} + F + K_AT_{1B})
\end{aligned} \quad [2]$$

As given by Wu, these coefficients are combinations of spin-lattice and spin-spin relaxation times (T_{1A}, T_{1B}, $1/R_{2A}$, $1/R_{2B}$), the first order rate constant for transfer of magnetization from pool A to pool B (K_A), and the "fully unsaturated" equilibrium longitudinal magnetization of pool B relative to pool A (F). M_A^Z is the longitudinal magnetization for spin pool A, and M_A^{Z0} is the "fully unsaturated" equilibrium value of this quantity; $\Delta\omega$ and ω_1 are the offset frequency and amplitude, respectively, of the saturating continuous wave (CW) radiofrequency (RF) with $\Delta\omega/2\pi$ and $\omega_1/2\pi$ typically given in KHz (7).

Nonlinear Constrained Optimization (NLCO) of Simulated MT Data Prepared by CW RF Irradiation

As can be appreciated after substitution of Eq. [2] into Eq. [1], this expression is nonlinear in the MT spin-system

Table 1
MT Parameters and NLCO Bounds

	T_{2A}	T_{1A}	K_A	F	T_{2B}	T_{1B}
CW simulation	62×10^{-3}	3.5	0.533	0.0239	25.0×10^{-6}	0.26[a]
Yeung and Swanson		3.0	3.0	0.09	60×10^{-6}	0.18
	R_{2A}[b]				R_{2B}[b]	
Egg white, minimum (NLCO)	1.0	0.5	0.19[c]	0.01	1.0×10^4	0.5
Egg white, maximum (NLCO)	1.0×10^3	10.0	7.6[c]	1.0	1.0×10^6	10.0

[a] Calculated from $FT_{1A} = Q/(1 - P/T_{1B})$.
[b] NLCO used rates (R_{2B}, R_{2A}) rather than time constants (T_{2B}, T_{2A}). Conversion to time constants was performed within the manuscript.
[c] Calculated via $K_AT_{1A} = Q/(P - Q)$ using T_{1A} maximum and minimum.

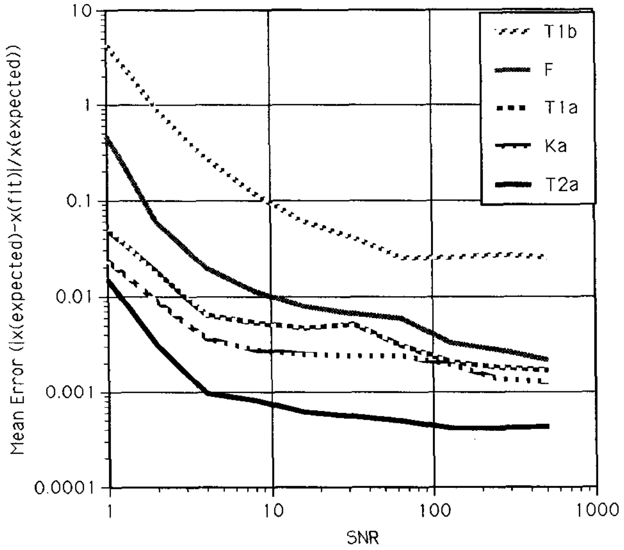

FIG. 1. NLCO was used to identify K_A, F, T_{1B}, T_{1A}, T_{2A} from simulated data Z-spectra, with variable SNR, from Eq. [1]. T_{2B} was estimated from the negative intercept of the simulated data as predicted in Eq. [6]. This parameter was then held constant for the NLCO. The mean error over the entire range of $\Delta\omega/2\pi$ (approximately 0–10 KHz) and ω_1 (approximately 0–10 KHz.) is shown as a function of data SNR. Attempts to determine all six spin-system parameters from the simulated data were unsuccessful, likely as a result of coupling between parameters. Note the high precision in the estimates of the parameters at reasonable SNR.

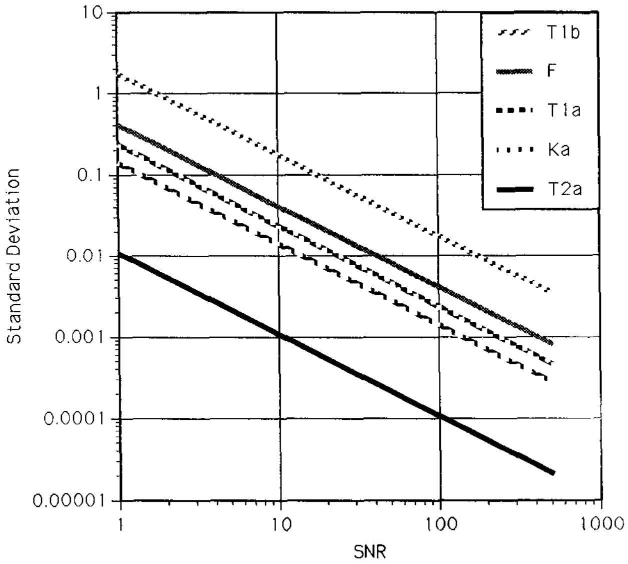

FIG. 2. The variance of each of the NLCO identified parameters was also determined over the offset and MT excitation amplitude range, as a function of SNR. This figure demonstrates the small variance used to identify K_A, F, T_{1B}, T_{1A}, T_{2A} from simulated data Z-spectra, with variable SNR. Here too, T_{2B} was estimated from the negative intercept of the simulated data as predicted in Eq. [6] and held constant for the NLCO algorithm.

parameters. Accordingly, we hypothesized that NLCO methods, similiar to those proposed by Gill *et al.* (4), would be appropriate for identifiying the parameters of this system. To test this hypothesis regarding MT parameter estimation, NLCO algorithms and Bloch-model simulations, as presented below, were executed using version 3.1 of MATLAB and its Optimization Toolbox (M-file = CONSTR.M; The Mathworks, S. Nattick, MA).

Representative MT spin-system parameters, shown in Table 1, were selected from the range of previously reported values (1–3, 8). Range constraints were used to ensure resonable parameter values: the constraints were based on theoretical limits (positive, finite) and literature reported predictions. Simulated Z-spectral data were generated using Wu's equation over a range of $\Delta\omega/2\pi$ from 0–10 KHz, and $\omega_1/2\pi$ varying from 0 to 1 KHz. Simulated gaussian white noise was added to provide a range of data signal-to-noise ratio (SNR) of 1 to 500. A simulated data set then consisted of several (e.g., 8) Z-spectra covering the ω_1 range specified above, at several (e.g., 8) $\Delta\omega$ values, also within the range specified above. Mean error and standard deviation of the estimated spin-system parameters were calculated using a Monte Carlo approach. One hundred randomly selected parameter sets, uniformly distributed within the parameter bounds (see Table 1), were each used to create a simulated Z-spectral data set: the data sets were then corrupted with gaussian white noise to vary the data SNR. One hundred different noise matrices were generated for each data set, and applied at 10 different SNR, for a total of 100,000 simulated experiments (100 parameter sets, 100 unique noise matrices/set, 10 levels/noise matrix). The estimated parameters were normalized to the expected value; the mean and standard deviation were then calculated over all experiments at each fixed SNR.

All simulations requiring identification of all six spin-system parameters failed to provide a unique solution, independent of the initial parameter vector (i.e., "initial guess"). However, setting T_{2B} to a known, "correct" value determined by an alternative procedure (3), allowed all remaining five parameters to be identified uniquely and accurately. Alternatively, fixing any one of the six parameters was sufficient to enable NLCO to uniquely and accurately estimate the remaining parameters–T_{2B} was chosen because a simple, efficient and independent method for its estimation (as briefly described below) has recently been identified (3, 6). Values of mean error and standard deviation of the parameter estimates are shown in Figs. 1 and 2, respectively, as a function of data SNR.

We also found that while NLCO uniquely determined the parameters (for the case of estimating five parameters), the precision of each can be shown to be dependent on the frequency offset and excitation amplitude used in the fit. This prompted us to directly look for the regions of data space that show significant dependence on each of the six basic parameters, via Jacobian analysis.

Jacobian Analysis

Estimation theory predicts that the best estimate, or "fit, for each parameter will be made over regions ($\boldsymbol{\Delta\omega}$, $\boldsymbol{\omega}_1$) of maximal sensitivity (5). The sensitivity of the Z-spectra with respect to the unknown parameter set $\theta = [T_{1A}, T_{1B}, K_A, F, T_{2A}, T_{2B}]$ can be determined from the Jacobian matrix,

$$J(Z, \theta) = \frac{\delta Z}{\delta \theta} = \left[\frac{\delta Z}{\delta T_{1A}} \frac{\delta Z}{\delta T_{1B}} \frac{\delta Z}{\delta K_A} \frac{\delta Z}{\delta F} \frac{\delta Z}{\delta T_{2A}} \frac{\delta Z}{\delta T_{2B}} \right] \qquad [3]$$

Using spin-system parameter estimates for boiled egg white albumin given by Yeung and Swanson (T_{1A} = 3.0 s, T_{1B} = 0.19 s, K_A = 3.0 s^{-1}, F = 0.09, T_{2B} = 60 µs (2), and a reasonable estimate for T_{2A} (62 ms), Figs. 3a–3f demonstrate each sensitivity term of Eq. [3], as a function of both nutation frequency and frequency offset, to the various spin-system parameters.

NLCO of Simulated Pulsed MT Data

Hardware restrictions of typical whole-body MRI systems (including ours), preclude CW MT RF excitation, and have led us to performing magnetization transfer excitation via shaped pulses (9). However, we have performed simulation studies that show near equivalence of steady-state longitudnal magnetization from CW and pulsed RF irradiated MT at similar power levels, above a threshold value for frequency offset (see Fig. 4, and (3, 6)). Therefore, although we expect significant differences in observed MT effects between the two excitation methods at low frequency offset (e.g., $\boldsymbol{\Delta\omega}/2\pi < \sim$2 KHz in Fig. 4), at midfrequency offset ($\sim$2 KHz < $\boldsymbol{\Delta\omega}$ < 10 KHz in Fig. 4) the differences are negligible. We also found, by additional simulations, that for this range the data is consistent with Grad & Bryant's assumption of negligible "direct" saturation (1). These values of $\boldsymbol{\Delta\omega}$ (and $\boldsymbol{\omega}_1$) are available on current commercial whole-body MRI systems. Note, however, that this range is not near the maximum sensitivity ranges for T_{1B} and F shown in Fig. 3 for CW RF irradiation experiments, indicating that these parameters may have relatively large imprecision in their determination by this approach.

Synopsis of Method for Determining T2B

Equation [1] transforms to Eq. [4] below when R_{2A} = 0 (i.e., an infinitely narrow linewidth for A), consistent with the assumptions of Grad and Bryant:

$$Z_{GB} = \frac{B'\omega_1^2}{2[D'\omega_1^2 + E'\Delta\omega^2 + H']} \qquad [4]$$

$$\begin{aligned} B' &= FK_A T_{1A} T_{1B} R_{2B} \\ D' &= FT_{1B} R_{2B}(K_A T_{1A} + 1) \\ E' &= E = FK_A T_{1A} + F + K_A T_{1B} \\ H' &= R_{2B}^2(FK_A T_{1A} + F + K_A T_{1B}) \end{aligned} \qquad [5]$$

By straightforward algebraic rearrangement of Eq. [4], we find the following linear relationship between the squares of the MT excitation amplitude ($\boldsymbol{\omega}_1$) and offset frequency ($\boldsymbol{\Delta\omega}$):

$$\Delta\omega^2 = \left[\frac{FK_A T_{1A} T_{1B} - 2Z_{GB}(K_A T_{1A} + 1)FT_{1B}}{2Z_{GB}(K_A T_{1B} + F + FK_A T_{1A})T_{2B}} \right] \omega_1^2 - R_{2B}^2 \qquad [6]$$

Equation [6] above is substantially different from the expression used by Grad and Bryant in at least two regards: a) it relates amplitude to offset frequency at any Z value, rather than just at half-max; and b) the intercept, which is used to calculate T_{2B}, is negative rather than positive. Thus, R_{2B} (and hence T_{2B}) can be estimated by plotting $\boldsymbol{\Delta\omega}^2$ as a function of $\boldsymbol{\omega}_1^2$ at different Z-values, and performing a regression on each of the data sets to obtain the "common" y-intercept.

New Analytic Expressions

Further algebraic manipulation of the coefficient of slope on $\boldsymbol{\omega}_1^2$ in Eq. [6] yields a second new analytic relationship,

$$m_n = \frac{FK_A T_{1A} T_{1B}}{2T_{2B}(K_A T_{1B} + F + FK_A T_{1A})} \left[\frac{1}{Z_n} \right] - \frac{FT_{1B}(K_A T_{1A} + 1)}{T_{2B}(K_A T_{1B} + F + FK_A T_{1A})} \qquad [7]$$

where m_n is the slope of $\Delta\omega^2$ versus ω_1^2 at a given Z_n value, with Z_n and other parameters as given elsewhere (1, 3).

Equation [7] can be further simplified to

$$m_n = \frac{Q}{2T_{2B}} \left[\frac{1}{Z_n} \right] - \frac{P}{T_{2B}} \qquad [8]$$

where Q and P can be measured from the slope and y-intercept of the regression line relating measured m_n at the known Z-$_n$ and T_{2B}; these new parameters are defined in terms of the spin-system parameters by

$$Q = \frac{FK_A T_{1A} T_{1B}}{(K_A T_{1B} + F + FK_A T_{1A})} \qquad [9a]$$

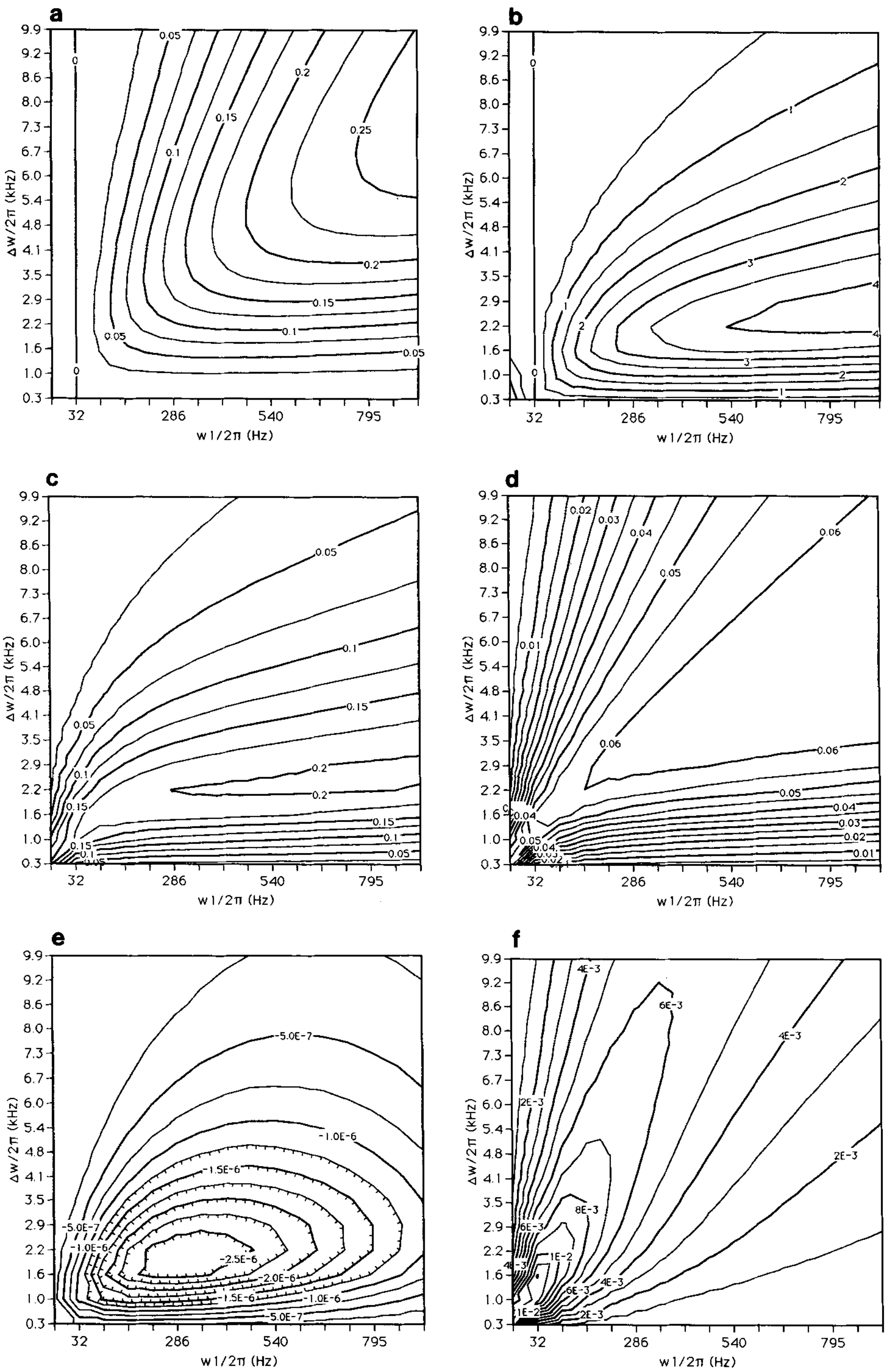

FIG. 3. The Jacobian provides a measure of the parameter sensitivity of a function, over a range of variables. This figure shows the six components of the Jacobian of Eq. [1] to the MT spin-system parameters, over the range of $\Delta\omega/2\pi$ (frequency offset) and $\omega_1/2\pi$ (RF amplitude) used in actual egg-white MT experiments in this manuscript. The sensitivity values were calculated by partial differentiation of Eq. [1] with respect to the individual parameters, followed by substitution of literature reported values for K_A, F, T_{1B}, T_{1A}, T_{2A}, and T_{2B}. The six components of the Jacobian are the sensitivities to: (a) K_A, (b) F, (c) T_{1B}, (d) T_{1A}, (e) R_{2B}, and (f) R_{2A}. Note that the maximum sensitivity of the parameters occur at different locations in ($\Delta\omega$, ω_1) space. There is no single location at which Eq. [1] is maximally sensitive to all parameters.

and

$$P = \frac{FT_{1B}(K_A T_{1A} + 1)}{(K_A T_{1B} + F + FK_A T_{1A})} \qquad [9b]$$

Although the two equations above (Eqs. [9a] & [9b]) are insufficient to uniquely determine the four remaining unknown parameters (i.e., F, K_A, T_{1A}, and T_{1B}, since R_{2A} has been assumed to be zero and T_{2B} is given as determined via an alternative method), they can be rearranged into two independent expressions describing some of the original six MT spin-system parameters

$$K_A T_{1A} = \frac{Q}{P - Q} \qquad [10]$$

and

$$FT_{1A} = \frac{T_{1B}Q}{T_{1B} - P} \qquad [11]$$

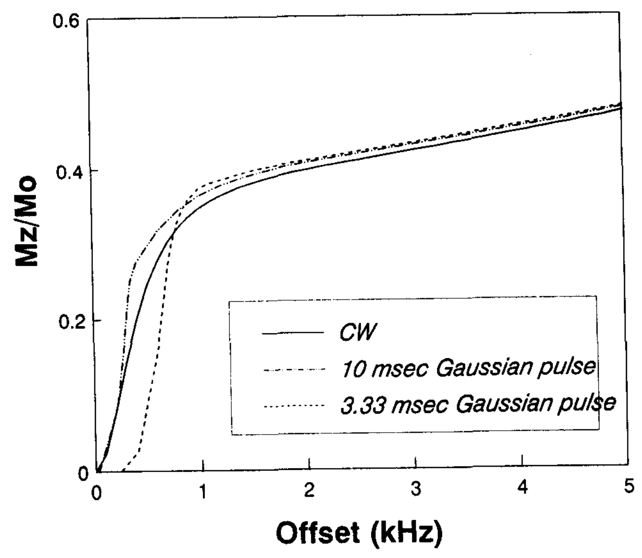

FIG. 4. Simulations were performed to compare pulsed and CW MT excitation over a range of $\Delta\omega$, two values of ω_1, and a fixed set of MT spin-system parameter values. Note that at low frequency offset ($\Delta\omega/2\pi < 2$ KHz) significant difference in predicted Z-spectra exist, yet at higher $\Delta\omega$ the differences become negligible. These differences suggest that the CW model of Eq. [1] and that of pulsed excitation are not sufficiently close at low $\Delta\omega$ to provide reasonable parameter estimation via NLCO. That is, pulsed MT excitation Z-spectral data will not match the modeled response predicted in Eq. [1], thereby preventing acceptable/valid parameter identification.

Requiring all MT spin-system parameters to be positive finite yields three additional algebraic relationships

$$T_{1B} > P \qquad [12]$$

$$FT_{1A} > Q \qquad [13]$$

$$\frac{F}{K_A} > \frac{(P - Q)T_{1B}}{T_{1B} - P} > P - Q \qquad [14]$$

Range boundaries for other parameters and combination of parameters can be estimated as described in Eqs. [10–15]. For the case of mid frequency range offset (i.e., where Grad & Bryant's Z-spectral approximation is valid, and where there is approximate equivalence of MT data prepared by CW and pulsed RF irradiation) only the two independent expressions relating the four spin-system parameters (Eq. [9]) can be uniquely determined. The Z-spectra are then fully described by a single linear expression with three spin-system parameters T_{2B}, P, and Q:

$$\frac{M_A^{\ Z}}{M_A^{\ Z0}} = 1 - \frac{QR_{2B}\omega_1^{\ 2}}{\Delta\omega^2 + R_{2B}^2 + R_{2B}P\omega_1^{\ 2}} \qquad [15]$$

Complete, perfectly specific saturation of pool B (10) can be calculated by evaluating Eq. [15] at very large ω_1,

$$\frac{M_{sat}}{M_0} = \lim_{\omega_1 \to \infty} \frac{M_A^{\ Z}}{M_A^{\ Z_0}} = \frac{1}{1 + K_A T_{1A}} = 1 - \frac{Q}{P} \qquad [16]$$

Thus, regression of the functional relationship (Eq. [8]) between the observed m_n and applied Z_n, together with the T_{2B} estimate obtained earlier by intercept of the $\Delta\omega^2/\omega^2$ regression line(s) (Eq. [6]), provides values of P and Q, from which the product $K_A T_{1A}$ and the saturation ratio M_{sat}/M_0 can be determined without actually measuring the system at saturation.

MEASUREMENTS ON EGG-WHITE USING A WHOLE-BODY MRI SYSTEM

Purpose

With the new understanding that the analytic relationships provide, we endeavored to: a) determine if the two pool Bloch model relationship predicted in Eqs. [6] and [8] is valid for the egg-white data; b) determine T_{2B} from the intercepts of regression lines fit as mentioned earlier; and c) test the application of NLCO and the new analytic expressions presented in the first half of this report.

Methods

Z spectra were generated for boiled egg white using 2DFT gradient echo pulse sequences with off-resonance, 10-ms duration, gaussian MT pulses, on a 1.5 T Picker VISTA HPQ whole body MR imager. The peak amplitude of the MT excitation pulse was varied, reaching a maximum value of approximately 1 KHz; offset frequency was varied and reached a maximum of approximately 10 KHz. A new data set was interpolated from this at nine values of Z were obtained ($Z_{n,n=1...9}$), ranging from 0.0775 to 0.1775, corresponding to M^z_A/M^{z0}_A ranging from 0.845 to 0.645. Data was then rearranged into sets of $\{\Delta\omega^2, \omega_1^{\ 2}\}$ data pairs for each value of Z_n. T_{2B} was determined from the intercept of a regression line, as suggested by Eq. [6] and fixed to this value during parameter optimization that followed. Other parameter optimization bounds were set as generous (± approximately one order of magnitude) windows around values from published reports while retaining positive finite characteristics (Table 1). Starting parameter estimates were taken from the literature (2) and 500 other random points within the bounds to assess the robustness (or uniqueness) of the parameter estimates. The constrained optimization algorithm (CONSTR.M) that was used (Version 3.1 of MATLAB with Optimization Toolbox, the MathWorks, Natick, MA) employs quadratic programming (4) to find optimal T_{2A}, T_{1A}, T_{1B}, K_A, and F for Eq. [1] above.

Due to expected differences between MT data produced by pulsed and CW RF irradiation (see Fig. 4), the minimum frequency offset data point included for analysis was systematically increased. This was done to investigate the effects of the two problems with low frequency data discussed earlier: a) MT data produced from pulsed RF irradiation is substantially different that resulting from CW RF irradiation, and b) pool A will in fact be subject to significant direct saturation (i.e., effects of the saturating RF irradiation pulses on pool A not mediated by pool B) at sufficiently low offset values. In the first set of fits, data at low values of $\Delta\omega$ were included with the $\Delta\omega$ starting point, then progressively increased to determine whether unique solutions to each parameter would be found. The minimum offset frequency data was then increased to determine whether there would be a point at which unique solutions to the parameters were no longer obtained. If unique spin-system parameters from the egg-white data were not found, the multiple sets of fitted parameters were evaluated for consistency with the relationships predicted in Eqs. [10–15].

The slope, m_n, of the linear relationship between $\Delta\omega^2$ and ω^2 at each Z_n (Eq. [6]) was determined by linear regression from the experimental data. Slopes used in this regression were from data restricted to $\Delta\omega/2\pi > 2$ KHz, based on visual inspection showing nonlinear behavior below this value (6).

A second linear regression was then performed, fitting $\{m_n, Z_n\}$ data pairs to Eqs. [7] and [8], yielding a slope $(Q/2T_{2B})$ and intercept $(-P/T_{2B})$ for this regression line. From the earlier estimate of T_{2B}, the parameters P and Q were calculated. M_{sat}/M_0 was then calculated from Eq. [16]. Relationships and ranges on parameters K_A, T_{1A}, F, and T_{1B} were estimated from P and Q, as described in Eqs. [10–14].

Results

Estimation of T_{2B}. The experimental data is plotted as $(\omega_1{}^2, \Delta\omega^2)$ data pairs at each Z_n, for fitting to Eq. [6], is shown in Fig. 8. The mean intercept was found to be -44.0 ± 2 kHz^2, corresponding to a T_{2B} of 24 μs ± 1 us. This value was then fixed and used in the five-parameter NLCO optimizations described above.

NLCO Parameter Estimation of Five Remaining Parameters. Variation of nonlinear constrained estimation of the experimental egg-white MT spin-system parameters in Eq. [1] as a function of increasing the minimum $\Delta\omega$ and the initial guess used in the analysis was substantial: 20-fold variation in T_{1B}, 4-fold variation in T_{1A}, 6-fold variation in F, 3.8-fold variation in K_A, and 8.4-fold variation in R_{2A}. Some of this variation resulted from nonunique solutions at $\Delta\omega/2\pi > 2$KHz. Figure 5a illustrates experimental data together with a theoretical prediction of the Z-spectral data based on parameters derived by NLCO. In this example, the NLCO used all of the available data to estimate the five spin-system parameters (with T_{2B} determined from negative intercept as described above, and held constant for optimization). Note that this theoretical Z-spectrum shows rather poor agreement, differing from the actual data by up to 22% over the range of $\Delta\omega$ and ω_1 used in these experiments, with an RMS error of 0.0178. Agreement between theoretical and experimental Z-spectra were equally poor for all of the initial guesses of the optimization (at low offset) despite unique parameter values.

When the minimum offset frequency data included in the NLCO was greater than 2 KHz, there was no unique parameter fit. Instead, the identified parameters were dependent on the initial guess provided to the NLCO, as noted above. Of the 500 attempted NLCO determinations, optimizations differing only in the initial guess for the parameter values, 127 optimizations found solutions within 1000 iterations of the NLCO procedure. The remaining 373 optimizations either failed to satisfactorally converge either because of becoming "trapped" at the edge of the parameter space, or simply failing to find a solution meeting the minimum error requirement within

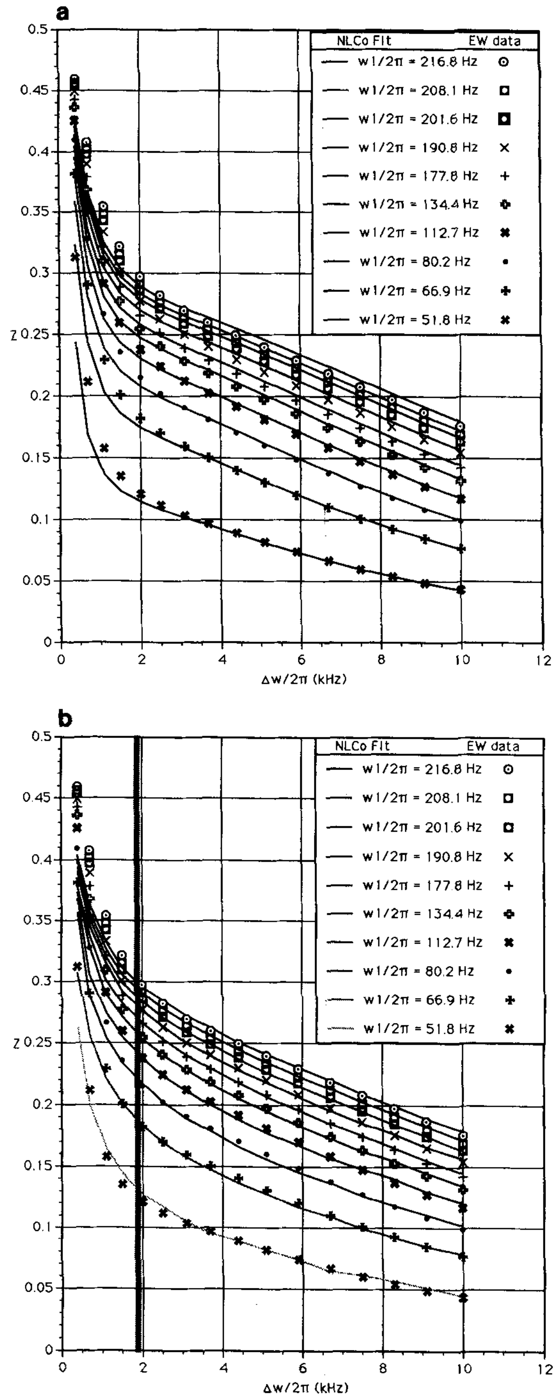

FIG. 5. The poor performance of NLCO parameter identification from pulsed RF irradiation data, when fitting to the modeled response given in Eq. [1], is shown here. Allowing the NLCO algorithm to evaluate all the available pulsed MT excitation egg-white Z-spectra, a unique set of spin-system parameters were determined (see Fig. 5a). (a) also shows the theoretically predicted Z-spectra (via Eq. [1]) compared with the actual data. Here, differences were below 22%, with an RMS error of 0.0178. Note that despite the unique NLCO parameter solution, a poor fit to the data is obtained, likely due to differences in the pulsed MT RF excitation and the CW model used in the "fit" to Eq. [1]. (b) Fitting the data over a restricted range of data (offset > 2 KHz led to substantially better fit: however, the parameter values were generally not unique.

the 1000 allowed iterations. No obervable patterns between the starting guesses in the NLCO and the ultimate NLCO success (e.g., convergence) were established. An illustration of the Z-spectra of a convergent parameter set is shown in Fig. 5b along with the egg white data. Although the egg-white data for $\Delta\omega/2\pi < 2$KHz were not used in the NLCO fit, they are displayed here to illustrate how the CW model diverges from the experimental data at low offset frequencies. The maximum error for the "fit" estimation of the egg-white data over the $\Delta\omega/2\pi > 2$KHz was 4.6% with an RMS difference of 0.00180: less than 1/10 that when parameter values were determined by performing NLCO over all available experimental data.

Figure 6 plots the product FT_{1A} versus T_{1B} for the 127 acceptably convergent parameter sets. The figure also includes the predicted relationship based on measurements of P, Q, and T_{2B} made with two different means: 1) successive linear regresssions based on Eq. [6] and [7], and b) fitting Eq. [11] to values of F, T_{1A}, and T_{1B} determined by NLCO.

Figure 7 shows the experimental egg-white data together with regression lines fitting this data to Eq. [6]. Low offset frequency data excluded from the fits (due to presumed direct saturation effects and differences between pulsed and CW RF irradiation experiments as discussed earlier) are not shown. Also included in this figure are theoretical lines based on spin-system parameters determined by NLCO. Note the excellent agreement between NLCO parameter predictions, regression lines, and experimental data. Errors between the experimental data (for $\Delta\omega/2\pi > 2$ KHz) and Eq. [7] or [8] using NLCO parameter predictions were less than 0.1%. Equally good fits were obtained for virtually all 127 convergent parameter data sets obtained by nonlinear constrained optimization.

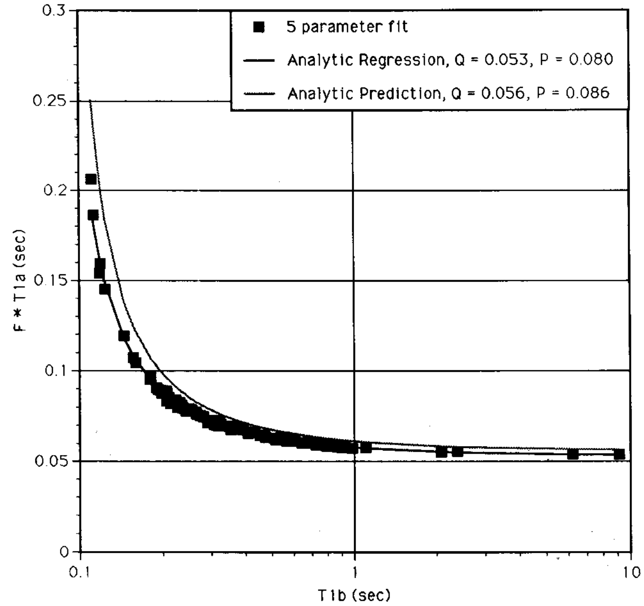

FIG. 6. Predicted relationship of FT_{1A} versus T_{1B} from Eq. [11], compared with nonunique, but successfully convergent NLCO estimates of the same parameters.

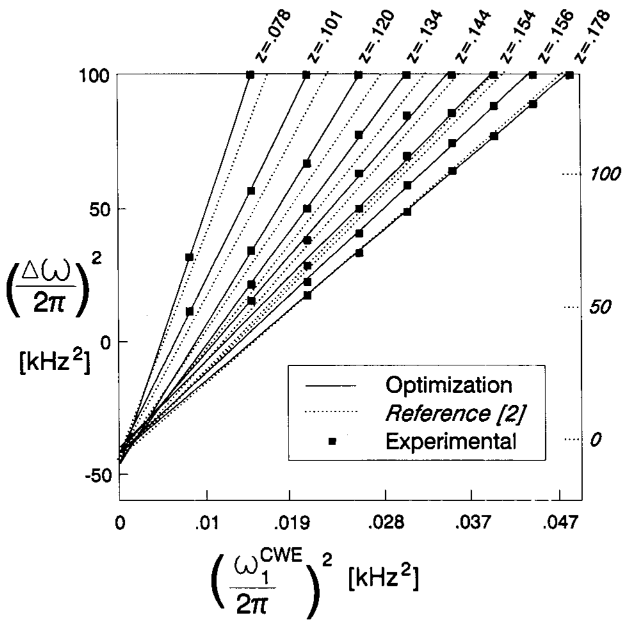

FIG. 7. Application of Eq. [6] to the pulsed RF MT egg-white data is presented. Closed boxes are the data used for the analysis: other points below $\Delta\omega/2\pi$ were excluded due to differences in pulsed and CW RF MT excitation, and due to direct saturation of the A-pool. Straight solid lines are least-squares fits of values of $(\omega_{1CWE})^2$ (defined below) and $(\Delta\omega)^2$ to Eq. [7]. Theoretical lines based on NLCO identified parameters, while not unique, overlie the regression lines. The dashed lines are the expected relationships based on MT spin-system parameters in ref. 2. Note that the NLCO optimization started its analysis from this starting guess, and moved to values providing better fits to our experimental data. In this figure, the $(\Delta\omega/2\pi)^2$ intercept is at −44 KHz^2, corresponding to a T_{2B} of 24 ± 1 μs. Here,

$$\omega_1^{CWE} = \sqrt{\frac{\int \omega_1^2(t)\,dt}{TR}}$$

as in ref. 5. This conversion is needed to ensure consistency with the analytic expressions that are based on CW excitation.

Application of New Analytic Expressions. Figure 8 shows a plot of m_n versus $1/Z_n$, testing the linear relationship predicted by Eqs. [7] and [8]. For this data, the linear regression correlation coefficient, R, is 0.9985; the remaining variation of the data may be due to experimental error in estimating ω_1^2 (6).

From experimental data on boiled egg white (3), values for P and Q were found to be 85.9 ± 3.7 ms and 56.2 ± 0.2 ms, respectively. M_{sat}/M_0 was computed at 0.347, consistent with a visual extrapolation of the saturation apparently due to MT (6). Thus, for this system T_{1A} has a lower limit of 85.9 ms, FT_{1A} must be greater than 56.2 ms, and K_AT_{1A} equals 1.89. The relationship between FT_{1A} versus T_{1A} is shown in Fig. 6 (along with that obtained from multiple NLCO analyses). Note that the maximum value of FT_{1A} cannot be determined without making assumptions concerning the minimum T_{1B}; the minimum value, however, is approximately equal to Q, or 56 ms ± 0.004.

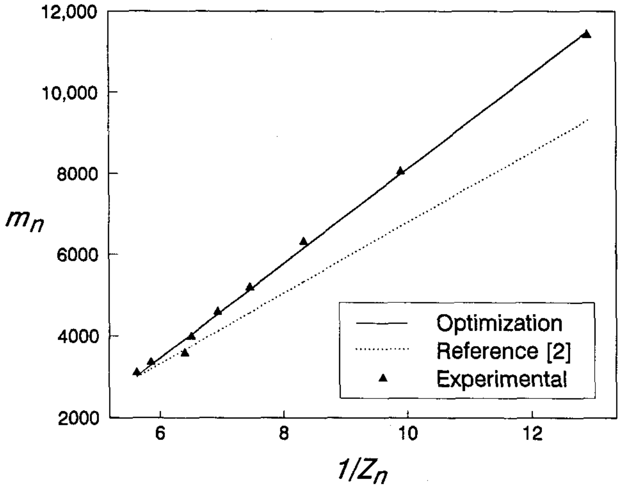

FIG. 8. Regression of the observed m_n at each Z_n and a knowledge of T_{2B}, outlined above, allows the egg-white MT spin system's P and Q to be determined, as described in Eq. [8] (solid line). Actual slopes, m_n, from the experimental data are shown as triangles. Here, P has been calculated to be 0.086, while Q has a value of 0.053. Range estimates and relationships between parameters have been determined from these parameters. The dashed line are the m_n values, as a function of $1/Z_n$ determined from the simulated MT experiments performed using MT spin-system parameters given in ref. 2.

DISCUSSION

Figures 1 and 2 demonstrate several important points. First, assuming that T_{2B} can be separately determined (1, 3, 6), the five remaining parameters can be individually and uniquely extracted from low- and midrange offset Z-spectral data resulting from CW RF irradiation via NLCO. That is, there is no coupling between these five parameters that would prevent determination of each parameter uniquely. Secondly, the parameters can be extracted with high accuracy and high precision at reasonable data SNR values. For example, the standard deviation of F is approximately 3% and the mean error is 0.1% at a SNR of 20. As seen by inspection of Fig. 1, the errors in the spin-system parameter estimates decrease with increasing data SNR; the variance of the estimate decreases similarly as shown in Fig. 2. These results suggest that Z-spectra resulting from CW RF irradiation, obtained at $1{,}000 < \Delta\omega/2\pi < 10{,}000$ KHz, and $0 < \omega_1/2\pi < 1{,}000$ KHz should be sufficient to identify all six MT parameters (T_{2B} via negative intercept, the remaining five from NLCO) with high precision for this hypothetical spin system. Note this also presumes the system is accurately modeled by a two-pool Bloch model with Lorentzian lineshapes. Note too, that errors in determination of T_{2B} (via any technique) will propogate through the optimization procedure; as such, care must be taken to minimize errors in its determination to avoid bias in estimation of the remaining parameters.

An important aspect of the Jacobian analysis (see Fig. 3) is that Eq. [1] is maximally sensitive to T_{1B} and F at relatively low offset frequency (well below 3 KHz). However, T_{1A} and K_A have larger ranges of maximal sensitivity, and include the mid-offset frequency range where the assumptions needed for our experiments (MT data from pulsed RF irradiation equivalent to that from CW RF irraditation, negligible direct saturation) are expected to be valid. There is therefore a fundamental difficulty in attempting to determine all of these parameters: there is no region of data space in which Eq. [1] is highly sensitive to all six MT spin-system parameters. This means that the accuracy of determination of each of the parameters will be differently affected by the availablility and accuracy of data at various positions in the data space. For example, accurate estimation of T_{1B} or F is possible at reasonable ω_1 values at *low offset* (well under 1 KHz for this spin parameter set); however, Eq. [1] is not sensitive to T_{1A} and K_A at these values, and their estimation would be poor if using data from only this region.

These differences suggest that it is important to consider the parameter estimation sensitivity and parameter relationships where available methods (e.g., pulsed MT excitation at whole body powers) prevent access to very low $\Delta\omega$ and high ω_1.

The parameter solutions including low offset data, while unique, do not provide "good" fits to the experimental data. In these cases, the NLCO algorithm has essentially found sets of parameters that optimally fit the data to Eq. [1]. Unfortunately, this frequency offset and excitation amplitude range is where we expect the largest differences between our experimental method (i.e., pulsed RF irradiation) and the CW conditions implied in Eq. [1]. Although the parameter values are unique, a rather poor fit to the experimental data is obtained, as illustrated in Fig. 5a (note error ranges provided in caption). Here, the model and data do not agree, yet a unique solution can consistently be obtained. Restricting the data used in the optimization to $\Delta\omega/2\pi > 2$KHz led to nonunique parameter values, yet an improved fit to experimental data as shown in Fig. 5b. This illustrates a common pitfall of "fitting" methods that do not also ensure that the model and data are consistent: in essence we can determine parameters that are mathematically reasonable yet physically meaningless.

Examination of the expressions containing the two uniquely determined parameters, P and Q (Eqs. [9–15]), shows that some of the six basic parameters are not uniquely determined by this mid-offset frequency data. For example, while the product of K_A and T_{1A} is known, explicit knowledge of one of these is needed to determine the other. A similar, but more complex relationship couples T_{1A} and F to T_{1B} (see Fig. 6). This figure also indicates that T_{1B} is sensitive to small changes in FT_{1A}; a system with this type of parameter behavior is often referred to as a stiff system. For example, when FT_{1A} approaches the asymptotic minimum (i.e., at 56 ms), if FT_{1A} varies by ±5%, then T_{1BA} varies by ±200%. Conversely, if T_{1B} approaches the asypmtotic minimum (86 ms), when T_{1B} varies by ±5%, then FT_{1A} varies by ±50%.

Previous studies have also noted that fitting of Z-spectral data may not be sufficient to unuiqely determine all MT parameters. Using an equivalent model and Z-spectral data of rat muscle, Caines *et al.* were able to uniquely determine three parameters (K, T_{1B}, and T_{2B}) by making assumptions about the other three parameters (f, T_{2A}, and T_{1B}) (11). Similarly, Henkelman *et al.* report that their fitting (of agar gel *Z*-spectra) does not provide a unique solution set (8). In general, confidence in finding "true" parameters, corresponding to a global minimum in optimization of a "true" model, is related to the accuracy of starting parameters and range estimates. Like any optimization process, this method would be improved by a) reducing the order of the function in the parameters, b) adding more constraining relationships between the parameters, and/or c) developing a more complete and accurate model for MT phenomena.

The relationships shown here place restrictions on MT spin-system parameter values based on slope and intercept measurements of transformed *Z*-spectral data. These algebraic relationships can be applied to MT experimental data for which the offset frequency satisfies the Grad and Bryant approximation. Besides fixing bounds on some fundamental parameters, an accurate value for M_{sat}/M_0 can be calculated; this provides a means for knowing if full saturation has indeed been achieved, as is presumed for the "standard" method of measuring K_A (10).

The validity of the Bloch model that underlies this analysis may reasonably be questioned, following the recent reports (7, 12). Henkelman *et al.*, (8) show a dramatic improvement in fitting agar gel MT data by replacing a Lorentzian lineshape (for the B pool) with a gaussian. Note, however, that the principal improvement shown there is seen at much higher offset frequencies than those used here, so that a Bloch model may be "phenomenologically sufficient" to describe the data presented here. The excellent fits of the data in Fig. 8 and to the predicted linear relationships (Eqs. [10] and [11]) provides experimental validation of the Bloch equation model for the midrange offset frequency. Note also that a gaussian lineshape is itself not a general solution (12); however, the overall better fit it may provide is leading us to consider further studies to test the applicability of the methods and results presented here to a gaussian lineshape model.

CONCLUSIONS

The new expressions and NLCO methods presented here offer new analytic techniques and insight for determination of MT parameters from *Z*- spectra. We found two specific sets of conclusions from our study, one each for MT data resulting from CW and pulsed RF irradiation.

First, from simulation results, it was found that all six MT spin-system parameters can be uniquely obtained with high accuracy via CW excitation obtained at low and medium frequency offset, accepted whole-body SAR and with reasonable SNR. Here, T_{2B} must be obtained by the "negative intercept" method presented here, or some other method, after which the remaining parameters can be determined by NLCO.

This approach cannot be applied to MT data from pulsed RF irradiation due to significant differences with CW RF produced MT data at low frequencies. However, because CW and pulsed RF application produces data that are quite similar at medium to high offset frequencies, expressions based on Wu's CW solution are applicable to data in this range. The parameter T_{2A} is effectively not represented by the data in this range, and so cannot be determined from it. We find that only T_{2B}, P, and Q in our treatment are sufficient to completely describe the *Z*-spectra in this range. The two parameters, P and Q, establish several limits and relationships on four parameters of the standard two-pool Bloch model (K_A, F, T_{1B}, T_{1A}), and also allow direct calculation of $M_{sat}{}^A/M_0{}^A$.

REFERENCES

1. J. Grad, R. G. Bryant, Nuclear magnetic cross-relaxation spectroscopy. *J. Magn. Reson.* **90,** 1–8 (1990).
2. H. N. Yeung, S. D. Swanson, Transient decay of longitudinal magnetization in heterogeneous spin systems under selective saturation. *J. Magn. Reson.* **99,** 466–479 (1992).
3. J. Hua, G. C. Hurst, Measurement of T_{2r} with a whole-body system. *J. Magn. Reson. Imaging* (1993). [SMRI Abstract #150]
4. P. E. Gill, W. Murray, M. H. Wright, "Practical Optimization," Academic Press, London, 1981.
5. L. Ljung, "System Identification: Theory for the User," Prentice Hall, Englewood Cliffs, NJ, 1987.
6. J. Hua, G. C. Hurst, Measurement of T2r via magnetization transfer *Z*-spectra. *J. Magn. Reson.*, accepted for publication, 1993.
7. X. Wu, Lineshape of magnetization transfer via cross relaxation. *J. Magn. Reson.* **94,** 186–190 (1991).
8. R. M. Henkelman, X. Huang, Q. S. Xiang, G. J. Stanisz, S. D. Swanson, M. J. Bronskill, Quantitative interpretation of magnetization transfer. *Magn. Reson. Med.* **29(6),** 759–766 (1993).
9. D. P. Flaming, W. B. Pierce, S. E. Harms, R. H. Griffey, Magnetization transfer contrast in fat-suppressed steady-state three-dimensional MR images. *Magn. Reson. Med.* **26,** 122–131 (1992).
10. S. D. Wolff, R. S. Balaban, Magnetization transfer contrast (MTC) and tissue water proton relaxation *in Vivo. Magn. Reson. Med.* **10,** 135–144 (1989).
11. G. H. Caines, T. Schleich, J. M. Rydzewski, *J. Magn. Reson.* **95,** 558–566 (1991).
12. H. N. Yeung, R. S. Adler, S. D. Swanson, Transient decay of longitudinal mangetization in heterogeneous spin systems under selective saturation–Part IV: Reformulation of the spin-bath model equations by the Redfield Provotorov Theory. *J. Magn. Reson.* accepted for publication, 1993.